F. Maggi, L.T. De Luca, A. Bandera
Pocket Model for Aluminum Agglomeration Based on Propellant Microstructure
AIAA Journal, Vol. 53, N. 11, 2015, p. 3395-3403
doi:10.2514/1.J053992

Pocket model for aluminum agglomeration based on propellant microstructure

Filippo Maggi[1] and Luigi T. DeLuca[2]
Politecnico di Milano, Milan, MI, 20156, Italy

Alessio Bandera[3]
IRTA S.R.L., Milan, MI, 20156, Italy

The propellant microstructure is addressed for the interpretation and the prediction of agglomerate size distribution in aluminized composite solid rocket propellants. Although the mixing process of a propellant is intrinsically random, repetitive fuel-rich local structures (pockets) are generated in the bulk. Pockets are privileged locations for agglomerate generation. In the present work second-order spatial statistics is applied to model-propellants for the characterization of the microstructure and for the definition of an agglomeration model. The model-propellants used in this work are generated by a packing code on the basis of real formulations, which are experimentally characterized for validation purposes. The average size and the metal content of the pockets are derived from the interpretation of the radial distribution function. The model is capable of predicting the size distribution of the incipient agglomerates for given propellant microstructures, using one free parameter for the tuning. The fitting of experimental agglomeration data from four different industrial propellants suggests that the free parameter can be expressed as a power function of the combustion pressure and that the microstructure agglomeration model produces particle distributions which reasonably match with the experimental data.

---

[1] Assistant Professor, Dept. of Aerospace Secience and Technology, 34 Via La Masa, AIAA member
[2] Retired Professor, Dept. of Aerospace Secience and Technology, 34 Via La Masa, AIAA Associate Fellow.
[3] Consultant

Nomenclature

Roman symbols

$\overline{R}$ = Mean pocket radius, μm

a = Vieille pre-exponential factor, $mm/s/bar^n$

$D[3,2]$ = Sauter mean diameter, μm

$D[4,3]$ = Mass-weighted mean diameter, μm

D_p = Pocket potential agglomerate diameter, μm

D_{agg} = Agglomerate diameter, μm

dr = Thickness of the shell in Radial Distribution Function (RDF), μm

g_{ij} = Partial RDF

N = Total number of particles in the pack

n = Vieille exponent

$n(r, dr)$ = Number of particles in a shell for RDF evaluation

N_p = Number of aluminum particles in pocket

N_{agg} = Number of aluminum particles collected by one agglomerate

N_i = Total number of particles of class i-th in the pack

r = Radius, μm

$R1$ = Radius of collection for agglomeration model

r_b = Burning rate, mm/s

R_{Al-l} = Radius of liquid aluminum agglomerate

V = Volume of the pack, μm^3

Greek symbols

ρ_{Al-l} = Density of liquid aluminum

σ_n = Standard deviation of variable n

I. Introduction

METAL fuels are commonly embedded inside composite solid propellants, in the shape of micrometric powders, with the scope of enhancing specific impulse performance, increasing density, and improving the combustion stability of the propulsion unit. A fraction of these particles tends to stick together at the burning surface and enters the gas flow in the shape of agglomerates, whose composition is mostly made by a mixture of molten metal and its oxide. Peculiar size and shape depend from the initial properties of the metallic ingredient [1]. The investigation on nano-sized aluminum, and metal fuels in general, unveiled the existence of multiple mechanisms of formation which are referred to the reactivity of the original powders and of the propellant. Flake-kind structures are generated from compositions containing nanoaluminum. Ammonium nitrate propellants produce large spherical agglomerates which can become as large as 1 mm, depending on formulation [2–4].

The containment of the agglomerate size represents a development driver for formulations improving the delivered specific impulse. The combustion of a metal drop is a relatively slow process whose duration can become comparable to the characteristic residence time inside the combustion chamber, if large agglomerates are present [5]. The expulsion from the nozzle of partially oxidized metal particles is a troublesome event leading to specific impulse losses. In addition, agglomerates are responsible for two-phase nozzle flow expansion and consequent performance detriment [6, 7]. The use of innovative fuels such as nanoaluminum, activated metal powders, boron-based compounds, or hydrides can lead to interesting performance benefits. Manufacturing, handling, and cost issues should be considered as well.

Current state-of-the-art composite space propellants are formulated mixing inorganic oxidizer, hydrocarbon binder, and micrometric aluminum powder. A three-dimensional heterogeneous microstructure is generated. The random placement of coarse oxidizer particles leave small fuel-rich regions filled by aluminum particles, polymer matrix, and fine oxidizer (if present). Small stripes of binder, called inter-pocket bridges, connect two neighboring and independent pockets [8]. A non-geometric representation of pocket microstructure is reported in Fig. 1(b). The originating heterogeneous propellant model is visible in 1(a).

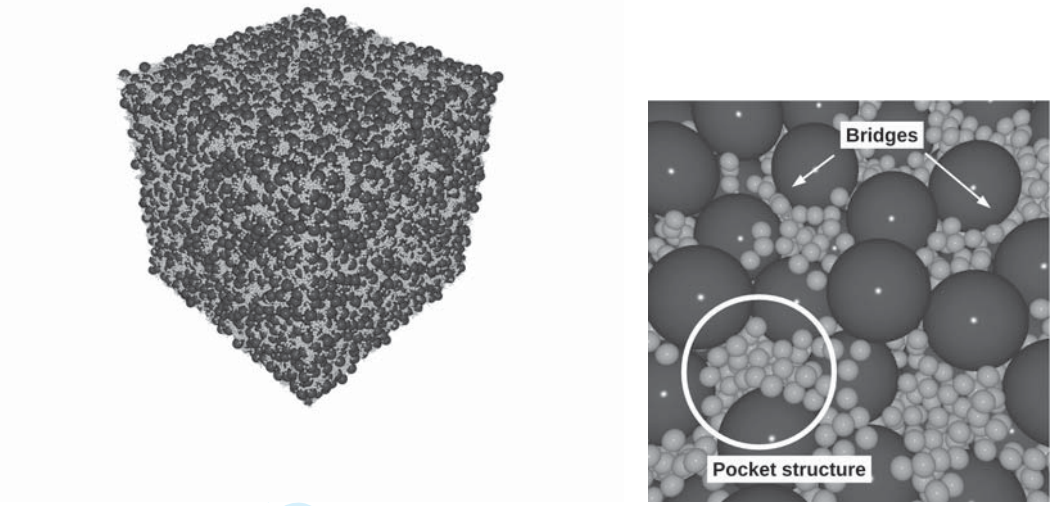

(a) Propellant pack (b) Detail of the microstructure

Fig. 1 Microstructure of a propellant model replicating an Oxidizer/Metal/Binder propellant (61/12/27 volume percent, 68/18/14 mass percent). Oxidizer size: 150 μm (dark spheres). Metal size: 30 μm (bright spheres).

The pocket structure was the subject of specific studies since the sixties and is considered a privileged location for agglomeration. Early experimental studies were performed by Povinelli and Rosenstein [9, 10]. Babuk worked on the problem through collection and measurement of condensed combustion products (CCP) generated from propellant formulations with varying oxidizer size [8]. In this respect, the SPLab research group has investigated this matter with both experimental and theoretical activities, as summarized in a recent paper [11].

It is possible to find in the literature several modeling efforts correlating particle arrangement and agglomeration. Geometric criteria were adopted by Cohen to get an estimate of pocket size and resulting agglomerates [12]. A recent model by Yavor *et al.* modeled the generation of agglomerates by evaluating the accumulation of metal at the burning surface, through a coupled mechanistic and geometric approach. A molten mobile layer is assumed at the burning surface, where the metal can accumulate. Its thickness depends on geometric features of the oxidizer particles [13]. The development of X-ray computed tomografy (XCT) techniques allowed the non-destructive inspection of propellant bulk but the application to agglomeration modeling was not straightforward [14, 15].

Spatial statistical tools were adopted for the characterization of propellant microstructure thanks to the availability of numerical models generated by packing codes, and correlated to experimental agglomeration data [16–19].

A microstructure statistical investigation and an agglomeration model based on propellant heterogeneity are presented in this paper. The work is based on the analysis of model-propellant representatives produced by a packing code [17, 20]. Statistical characterization of the pocket size is addressed, showing the sensitivity of this property from the domain. An agglomeration model is developed on the basis of this theoretical framework, supported by an experimental data set.

II. Aluminum agglomeration

Agglomerates are mostly originated by the aggregation and melting of neighboring metal particles, once they reach the burning surface. Aluminum is warmed up by the heat feedback from the flame and from local reactions. Nearby particles start sticking together in filigree-kind shapes. As the hottest regions of the flame get in contact with this irregular structure, metal temperature rises, inflammation occurs, and the aggregate collapses into one fused drop. If external acceleration fields are absent, the agglomerate detaches from the burning surface once the lifting forces from gaseous products of solid phase decomposition overcome the retaining ones. High speed visualizations reported in Fig. 2 reproduce experimentally, for a metalized propellant based on (AP) and hydroxyl-terminated polybutadiene (HTPB), the description that was given by Price [1]. In the present work only standard micrometric aluminum is considered but it is acknowledged that different chemical and physical nature of the metal fuel may change local reactivity, altering the aggregation-to-agglomeration process [2–4].

Pocket structures are locations where agglomeration is favored by contemporary coexistence of specific local conditions and metal particle proximity. The core of a pocket contains an oxidizer-lean mixture of fine AP powders, if any, and polymer binder which are decomposed by the heat feedback from the flame region. Fuel vapors and oxidizing gases mix together and react promptly, being this oxidizer very fine (in the order of few microns). This flame is not very hot though, because the oxidizer-to-fuel (O/F) ratio is unbalanced with respect to the stoichiometric value. A typical

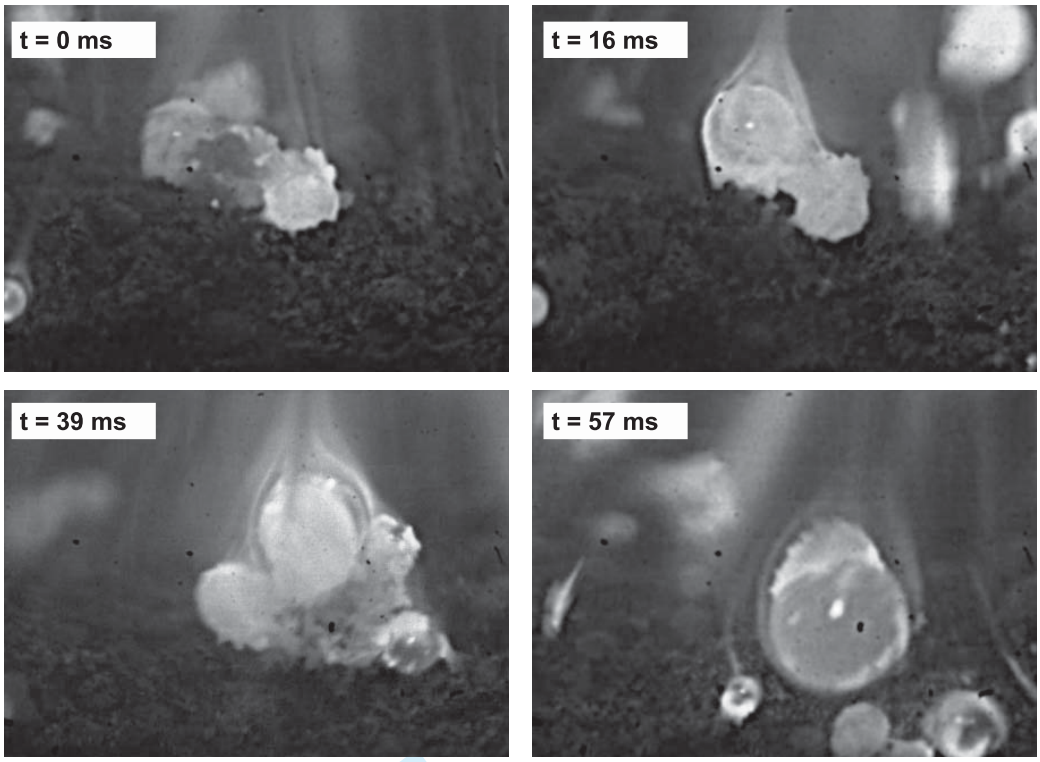

Fig. 2 Agglomeration sequence of an aluminized AP/HTPB propellant at 5 bar. Size of image view is 1.75 x 1.25 mm.

aluminized formulation is reported in Table 1, as a matter of example. This propellant embeds a blend of 200 μm size and 10 μm size AP. Inside the pocket, only the fine AP cut, aluminum, and HTPB can enter. If we assume that micrometric aluminum emerging from the bulk heats up and melts, but does not contribute to combustion, the local adiabatic flame temperature is around 1000 K (see Fig. (3)). The coarse AP lays at the borders of the pocket. Its decomposition and

Table 1 Formulation of propellant A. The density of cured HTPB is 920 kg/m^3.

Material	Size, μm	Mass fraction, %	Volume fraction, %
AP	200	58	52.41
AP	10	10	9.04
Al	30	18	11.75
Binder	—	14	26.81

reaction with the rest of the components (excluding aluminum) would produce an adiabatic flame

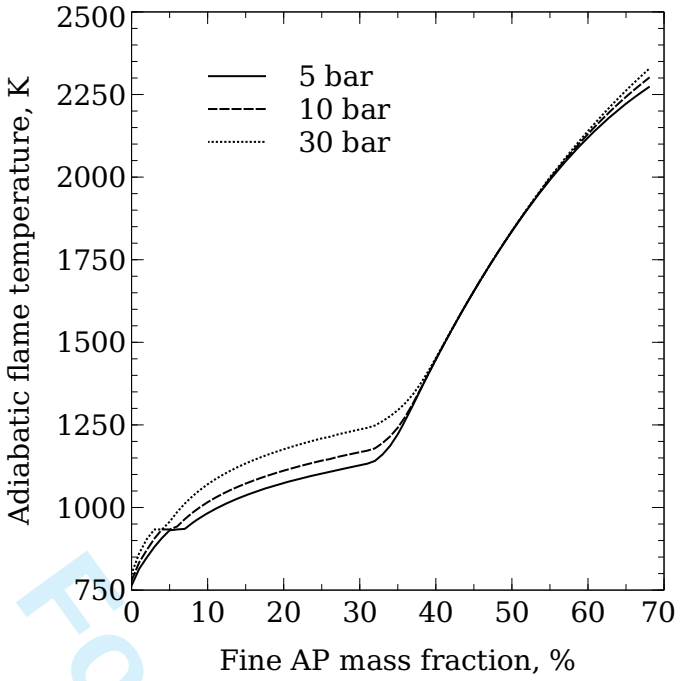

Fig. 3 Adiabatic flame temperature of pocket content as a function of fine AP mass fraction, with respect to a reference composition containing 68% of AP, 18% of aluminum and 14% of HTPB. Only fine AP, HTPB, and nonreactive aluminum are considered [21].

temperature of 2700 K but the complete mixing of the reactants can occur only some tens or even hundreds of microns above the burning surface. This scenario is represented in the multiple flame model by Beckstead, Derr, and Price [22].

As long as the micrometric aluminum remains inside the pocket region, it appears that metal melting can occur, if a minimum amount of fine AP is present. Local temperature does not suffice for ignition. Experimental tests by Trunov and co-authors found that the ignition of micrometric powders occurs when the natural oxide coating can melt, at about 2300 K [23]. Some contrasting data can be retrieved in the Russian literature. In a review by Pokhil *et al.* the reader can find much lower temperature values for particle ignition in active media, as low as 1300 K, in presence of the high oxidizer concentrations typical of AP-based propellant combustion. Sourced papers were originated by different authors, under various flow conditions and initial particle sizes [24]. Experimental outcomes reported in a paper by Mullen and Brewster support the idea that agglomeration is influenced by the local temperature. The authors developed some propellants

granting minimal agglomeration by tailoring the pocket composition [25]. If the size of aluminum powders is decreased to the nanometric region, a different aggregation-to-agglomeration process was captured through high-speed visualizations by the SPLab-POLIMI group. Combustion surface magnifications showed bright, thin flake-kind aggregates building up and detaching from the burning surface [2]. The generation of spherical agglomerates at the burning surface was not evident. This class of materials was observed to ignite in air at a relatively low temperature. Dossi *et al.* found ignition temperatures around 800 K for particles in the order of 100 nm size [26]. Unlike the micrometric aluminum, those nanoparticles may be capable of some local reactivity inside the pocket, causing a different agglomeration behavior. For this reason, a common modeling approach for both micro- and nanoluminum does not seem to be suitable.

The present paper deals with the peculiar agglomeration process of AP-HTPB-Al propellants embedding micrometric aluminum powders. Three different attitudes were classified by Babuk, related to propellant type and combustion conditions [8]. The *subpocket* agglomeration occurs when burning rate, and thus pressure, is relatively high. Under such conditions, the reduced residence time does not allow complete agglomeration, favoring the release of multiple agglomerates from a single pocket. On the contrary, a slower burning rate expands the average residence time, thus enabling the whole metal in the pocket to take part in the formation of one agglomerate (*pocket* agglomeration). Finally, in some cases the agglomerate does not leave the surface but collects other siblings, moving across the propellant surface through the interpocket bridges (*interpocket* agglomeration).

III. Pocket characterization

When particles arrange randomly in space some replicating structures at microscopic level are formed. Spatial placement of particles follows well defined paths that depend on size, shape, and coarse-to-fine ratios. The final packing fraction is strictly dependent on the interaction of these features [28].

Characterization and measurement of pockets is of primary importance for the analysis of the agglomeration. The local structure can be investigated through spatial statistics, using functions of different order. First-order statistics corresponds to probe a mean volumetric property (e.g. the

density). Higher-order statistics characterizes the particle-particle reciprocal position and enables the quantification of average geometric features of the matter [29–32]. A second-order statistical approach is proposed in this work.

A. Dimension of pocket

In previous papers the authors showed that agglomeration process could be correlated to the pocket size through higher order statistical descriptors [11, 18, 31]. The radial distribution function (RDF, a.k.a. pair-correlation function) belongs to the family of second-order statistics. A practical algorithm to implement the function consists of drawing a shell of radius r and thickness dr around a center-point reference particle. The number of item centers that are located within this defined control volume are counted. The procedure is iterated throughout all the particles. The function $n(r)$ represents the mean value of such operation for a given radius, which is incremented till an asymptotic behavior is approached (Fig. 4). The RDF consists of the ratio between the particle number density in the local shell and in the whole volume. If the population contains different particle types, the RDF can be specialized to analyze the reciprocal position of one family with respect to another (partial pair correlation function). The RDF for aluminum-aluminum particle analysis, defined in Eq. (1), can be used to highlight the attitude of the metal fuel to generate clusters within the bulk of material, prior to combustion [18].

$$g_{Al-Al}(r) = \frac{V}{N_{Al}} \frac{n(r)}{4\pi r^2\, dr} \tag{1}$$

The symbol V refers to the volume of propellant which contains the number N_{Al} of aluminum particles. The ratio N_{Al}/V is called intensity. This kind of algorithm is prone to parallelization with shared [33] as well as distributed [34] memory models and demonstrated higher scalability with the former paradigm.

The partial pair correlation function can be used for the measurement of mean pocket size. This function analyzes the surroundings of all metal particles at a given distance and suggests whether the presence of metal is less than the average (g_{Al-Al} <1) or more than the average (g_{Al-Al} >1). An aluminum pocket is bounded by AP particles and inter-pocket bridges which contribute to generate a surrounding region where metal population is lower than the average, thus featuring

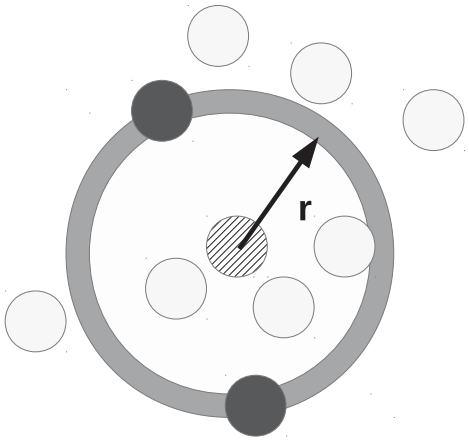

Fig. 4 Evaluation of parameter $n(r)$ for one reference particle (dashed) and one radius. Only dark particles are counted by the function.

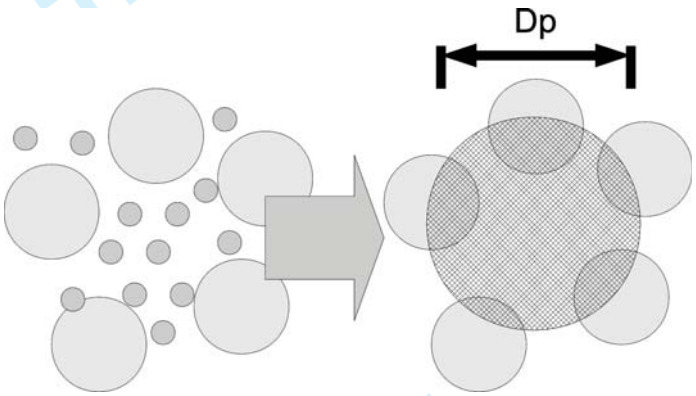

Fig. 5 Representation of the pocket diameter. Coarse oxidizer (in bright color) confines groups of metal particles (in darker color).

g_{Al-Al} <1. Unlike in Cohen's model, the border of the pocket is defined by the random particle-particle arrangement and not by a geometric construction (Fig. 5). The value of the RDF identifies a mean property of the matter which results in a smooth transition between inner and outer side. That is, the pocket size is conventionally identified in the minimum of the function, in the interval where the RDF value is below the unity.

Data variability and representativity of the statistical analysis should be considered. Composite propellants are made by three-dimensional random arrangements of smaller items. If sample size is large enough, the fluctuations of the local properties do not influence the global features and their statistical representation. Different samples with identical compositions should lead to identical

results. Conversely, if the sample is small, the average statistics can be influenced by the local structure. In the latter case, a single characterization cannot be considered a good representation of the mean behavior and multiple runs should be performed to reduce potential data scattering. The reader can find some affinity with experimental investigations. In order to show the variability connected to heterogeneity, Propellant A model is packed with particle number ranging from 31250 to half million, using a random packing code based on Lubachevsky-Stillinger algorithm [17]. The fine AP cut is homogenized into the binder for a matter of computational time, leading to a simulated volumetric packing fraction of 64.15% [35]. Three samples per each cubic pack were produced by changing the initial random seed. Pocket size was determined through the RDF function of Eq. 1. Details of the results are given in Table 2. Figure (6) reports the statistical confidence intervals. The average pocket size is quite reproducible, featuring a difference below ±1%. The standard

Table 2 Mean pocket size in a random cubic pack reproducing propellant A. Averages and standard deviations are evaluated on a data set of three different packs.

Pack id.	N	N_{Al}	N_{AP}	Pack length, mm	$\overline{R}$, μm	$\sigma_{\overline{R}}$, %
A1	500000	492583	7417	3.90	162	2,04
A2	250000	246291	3709	3.09	162	1,35
A3	125000	123146	1854	2.45	160	3,52
A4	62500	61573	927	1.95	162	5,81
A5	31250	30786	464	1.55	159	8,19

deviation of $\overline{R}$ in the single packs can increase above 5% as the number of the coarser cut is reduced to 1000 particles. The reader should easily understand that the use of one pack as a propellant representative can lead to a statistical error, which can be reduced if the particle number of the model is incremented. When the use of one large pack is prohibitive from a computational point of view, the accuracy of the statistical representation benefits from multiple runs. The number of tests should be a matter of a trade-off evaluation, as in the case aforementioned.

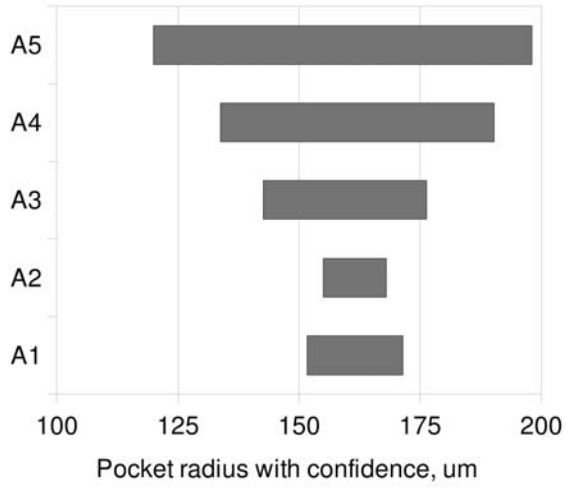

Fig. 6 Pocket radius of propellant A with interval of confidence. Six-sigma criterion is adopted. The uncertainty on detected pocket size increases as the number of particles in the pack is reduced.

B. Metal content of pocket

Once the pocket size $\overline{R}$ is computed, the metal content is defined by Eq. (2).

$$N_p = \int_0^{\overline{R}} n(r) dr' \tag{2}$$

N_p is the mean number of particles in the pocket. Past investigators tried to correlate the average metal content of pockets to the experimental agglomerate size [18, 19]. The mass of aluminum in the pocket m_p is the sum of the contributions from each particle. The diameter D_p of an equivalent agglomerate can be computed by Eq. (3). We will refer to this ideal condition with the name of *potential agglomerate*. Liquid aluminum density ρ_{Al-l} is assumed in this work because all experimental data of this paper refer to incipient agglomeration status, just after the release of the molten particle in the gas phase.

$$D_p = 2 \left(\frac{3}{4\,\pi} \frac{m_p}{\rho_{Al-l}} \right)^{1/3} \tag{3}$$

Mean pocket metal content is subjected to fluctuations across different propellant samples, following the heterogeneous nature of the propellant. Table 3 reports average data for both pocket content and potential agglomerate diameter for the model-propellants A1 to A5. Three runs were analyzed per each case. The σ_{Np} can be as high as 20% for the smallest propellant packs. Fluctu-

ations of D_p are lower, featuring a standard deviation of 7%. The variability is smoothed out for packs A1 and A2, where standard deviation reached a minimum. In this respect, the pack A3 is not yet fully satisfactory and represents a compromise between precision of the methodology and computational costs.

Table 3 Mean pocket metal content and potential agglomerate size in packs of Propellant A.

Pack id.	N_p	σ_{Np}, %	D_p	σ_{Dp}, %
A1	156	5,2	168,1	1,8
A2	156	3,4	168,2	1,1
A3	151	9,2	166,4	3,0
A4	158	14,6	168,6	5,0
A5	150	20,2	165,6	7,0

C. Potential agglomeration: experimental considerations

The experimental characterization of incipient agglomeration was performed for propellant A. Some hundreds of agglomerates were measured after the release from the combustion surface by means of a consolidated optical technique based on high-speed camera visualizations and long-range microscopy [11]. The current experimental procedure enables measurements of items as small as 30 μm, for combustion occurring in the range 5 to 40 bar. The conditions may be more stringent if the propellant is more reactive (e.g. in presence of nanoaluminum). Data presented in this paper are limited to 25 bar and threshold diameter is set to 50 μm for consistency among different tests, unless differently stated. Table 4 reports the resultant mass-mean diameter as a function of pressure. The estimated number of initial metal particles which contributed to the formation of the experimental mean agglomerate is reported as well. Metal combustion is disregarded, resorting in a mere geometric approach. Limiting assumptions consider that condensed products are in a final liquid state, that aluminum oxide fraction is negligible at this stage of the combustion, and that initial aluminum is spherical of 30 μm diameter.

The microstructure of propellant A was simulated with a half million particle pack. The average pocket size was $\overline{R} = 162\mu m$ and the mean number of aluminum particles available for the

Table 4 Experimental agglomeration data as a function of pressure for propellant A. Mean number of particles in pocket is $N_p = 157$ (derived from heterogeneous model).

p, bar	D_{agg}	N_{agg}
5,0	263,8	601
10,0	266,0	616
20,0	167,1	153
25,0	141,9	93

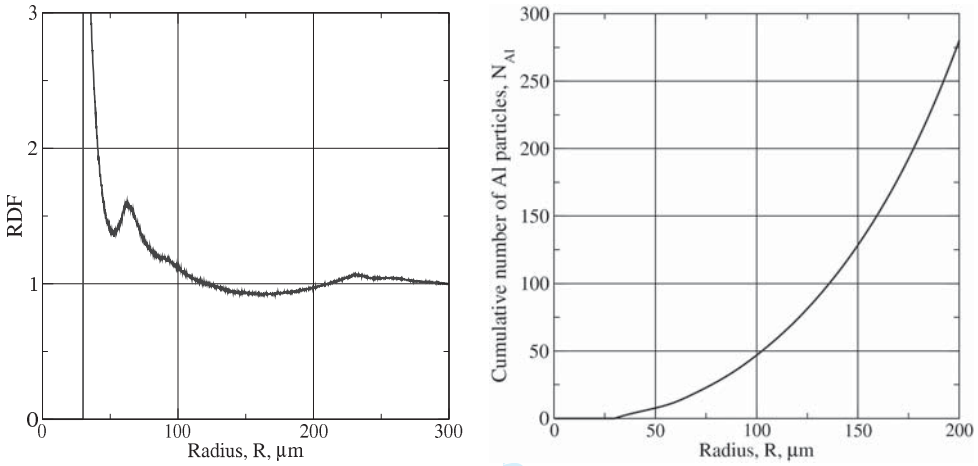

(a) RDF (b) Number of aluminum particles

Fig. 7 Second-order statistical characterization of propellant A1. The RDF and the mean cumulative number of aluminum particles are reported.

generation of a potential agglomerate was $N_p = 157$ (Figure 7). From the comparison of model data with experimental outcomes of Table 4, it is clear that agglomeration cannot be fully predicted by analyzing the sole pocket region. This result is in line with past works which used similar geometric approaches [36]. The comparison of N_p and N_{agg} suggest that aluminum is collected beyond the border of a pocket, when low pressure combustion occurs. In the case under examination, for the tests at 5 and 10 bar, the metal content of about 4 pockets is necessary to create the average agglomerate size. This number may be slightly overestimated since inter-pocket bridges are not fully considered. Conversely, the number of collected particles is progressively decremented if pressure is increased. At 20 bar it appears that the whole pocket participates to agglomerate formation while,

at higher pressure, only a fraction of aluminum contained inside the pocket is captured. The same concept was expressed by Babuk when he referred to subpocket, pocket and interpocket regime of agglomeration. Such considerations are valid for the observed case but can be extended to other compositions based on micrometric aluminum and inert binder, after specific experimental analysis and pressure dependence investigation.

IV. Agglomeration Model

Pocket metal content and potential agglomerate size represent an average geometric feature of the propellant, disregarding combustion dependence. At the same time, visualizations of the burning surface performed during this activity and the past works by Babuk or Povinelli demonstrated that the microstructure maintains rather important role in superficial evolution of aluminum. The agglomeration model here described aims at condensing into one framework both the geometric features of propellant heterogeneity and the combustion dependence, using a tuning parameter.

A. Description

The model refers to the prediction of incipient agglomeration and necessitates the availability of a propellant numerical representative, generated by a packing code. At every iteration, one metal particle is randomly selected in the pack to become the center-point of an agglomerate. A spherical region of collection is defined around it and the radius of this domain is called *radius of collection* ($R1$). Aluminum particles which are contained in the region are supposed to collapse into the agglomerate (Figure 8). When particles are captured, they are removed from the pack and cannot contribute to other agglomerates. After this operation, random sampling identifies a new reference particle and the respective region of collection. The algorithm is repeated till the whole metal content of the pack is processed. This sequential algorithm produces a list of agglomerates on the basis of microstructure properties and the parameter $R1$. The center-point of an agglomerate may be selected everywhere in the pack. If it is located in an inter-pocket bridge or in a region where few particles are still available, the resulting agglomerate will be small. On the contrary, a larger collection will result. In any cases, the probability that the center-point is selected within a pocket is higher because of the local number density. Everything is based on the assumption that,

at each iteration, every available metal particle in the pack has the same probability to be selected as a new center-point. It follows that specific functions for long period generation of pseudo-random numbers are highly suggested. This work adopted the Mersenne-Twister algorithm implemented in the GNU Scientific Libraries [37].

The radius of collection is the only free parameter of the model and can introduce a pressure dependence on agglomerate size prediction. When $R1$ is changed, the region of collection of each agglomerate varies accordingly. For $R1 < \overline{R}$, the region of collection is smaller than the pocket structure, producing the subpocket agglomeration regime. This feature is typical of fast-burning propellants and high-pressure combustion. On the contrary, for $R1 > \overline{R}$ the collection region is beyond pocket borders and interpocket agglomeration is attained, corresponding to slow burning rate and low combustion pressure.

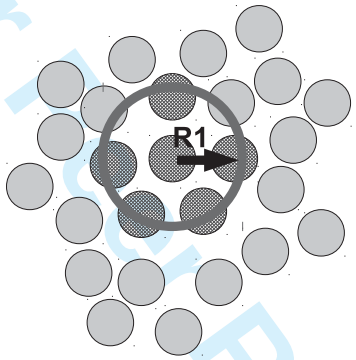

Fig. 8 Scheme of the model. Particles within the region of collection collapse into one agglomerate.

A test for parameter sensitivity on propellant pack A1 is shown in Figures 9 and 10. The value of $R1$ is incremented beyond the limits of pocket diameter, that in the specific case is $D_p = 168.1\mu$m. A cutoff on predicted particle sizes is applied at 50 μm, in agreement with the specific experimental data set. Density of liquid aluminum is assumed.

Larger agglomerates are obtained, increasing the radius $R1$. Monomodal or bimodal agglomerate populations are generated for the tested propellant and the investigated range of the parameter. It is important to underline that the model is still based on spatial statistics and does not include a combustion model for aluminum. Smoke prediction is not possible and the minimum size of the

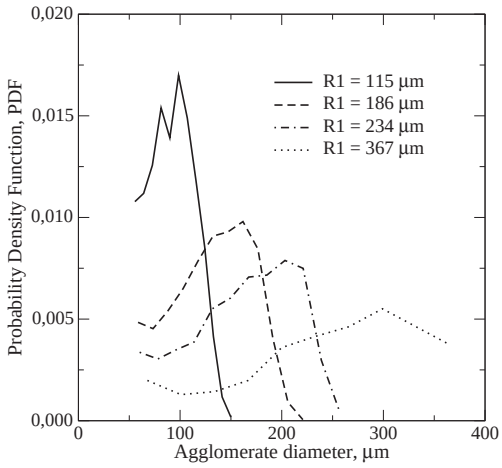

Fig. 9 Parametric test of PDFs for agglomerate size distributions, generated from propellant A1 by different values of $R1$. The pocket radius computed for the specific pack is $D_p = 168.1\mu$m.

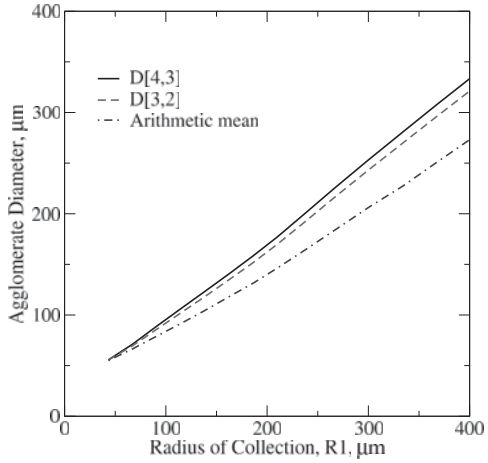

Fig. 10 Parametric test of mean agglomerate diameters originated from propellant pack A1, as a function of $R1$. Computed pocket diameter is $D_p = 168.1\mu$m.

combustion products cannot be smaller than one single aluminum particle. Nevertheless, this fact is neglected since the experimental measurement technique observes the agglomerates right after the detachment from the surface, minimizing the effect of metal combustion.

B. Fitting to experimental data

Incipient agglomeration is analyzed for a series of propellants. Formulations A (already mentioned in this paper), B, and D are industrial batches while formulation C is a lab-scale preparation.

Numerical microstructure models are generated on the basis of the respective nominal formulations. Details are listed in Table 5. Propellant A is here repeated for convenience. Four classes of particles are simulated (400 μm, 200 μm, and 150 μm for the oxidizer and 30 μm for the fuel). AP fine cut (about 10 μm) is homogenized into the binder. Propellant ballistics and incipient agglomeration data are retrieved from high speed and high resolution video recordings. Combustion tests are conducted inside a vessel, pressurized with nitrogen. The experimental rig is equipped with a closed-loop control system that ensures constant pressure during tests. Combustion videos are elaborated by the in-house software *Hydra* for automatic burning rate digital post-processing. Regression data are fitted to the Vieille law $r_b = a\, p^n$. Table 6 reports the interpolation curves in the relevant pressure ranges.

Table 5 Nominal compositions of propellants and number of particles used for their simulations.

Id	AP 400 μm	AP 200 μm	AP 150 μm	AP fine	Al 30 μm	Binder	N
A	0	58	0	10	18	14	500000
B	0	55	0	14	19	12	500000
C	0	0	68	0	15	17	300000
D	32	24	0	13	19	12	650000

The proposed agglomeration model is used to address the relation between experimental agglomerate size, heterogeneous propellant microstructure, and combustion pressure. Once experimental agglomerate distribution is derived from burning tests (Figure 11), model predictions are compared. An iterative procedure is originated to find the value of $R1$ which grants the matching between predicted and experimental mass-mean diameter. A simple root-finding algorithm is applied. Only one solution is found for $R1$, being a monotonic dependence. The analysis is repeated for each available combustion recording, obtaining a series of $(p, R1)$ couples. Finally, data are fitted using a power law $R1 = z\, p^q$ (Figure 12). Correlations are reported in Table 6, along with the statistical characterization of the heterogeneous microstructure.

Tested propellants feature relatively similar behavior. Ballistic exponents of the Vieille's law fall

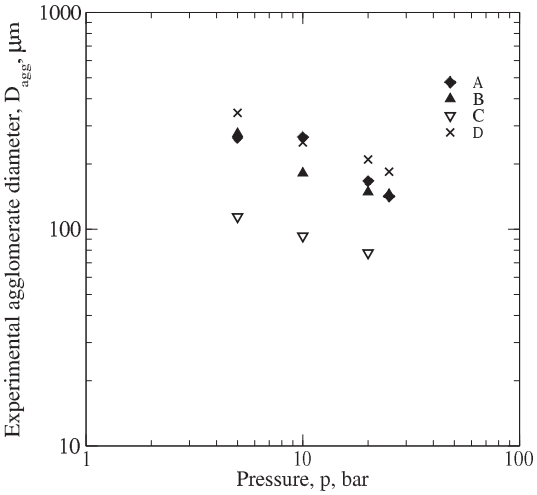

Fig. 11 Experimental mean diameter size D_{agg} of agglomerates generated by propellants listed in Tab.5.

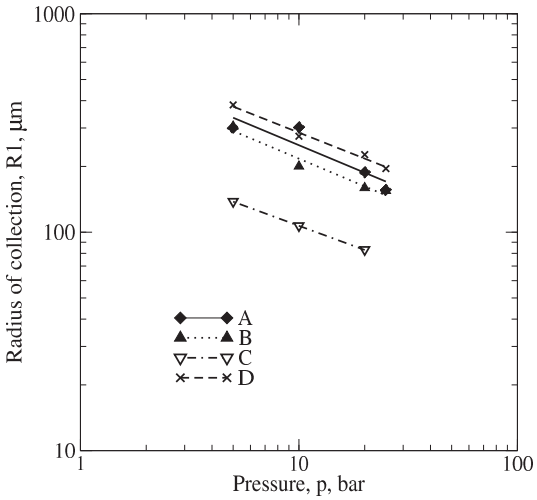

Fig. 12 Fitting of $(p, R1)$ couples obtained by comparison between experimental and model data for propellants listed in Tab.5.

in the range 0.40-0.49. Propellant A and B have similar microstructure, testified by the value of the radius $\overline{R}$. Coarse oxidizer dispersion dominates the arrangement of particles and fine AP becomes part of the pocket. Propellant C takes advantage of the reduced oxidizer size. The pocket extension is decreased and the burning rate is incremented. Propellant D contains the coarsest oxidizer (400 μm) and has a bimodal AP distribution. It tends to burn slower with respect to other formulations and features the largest pocket structure , from the geometric viewpoint. Out of the tested group, propellants A, B, and D, demonstrate higher level of agglomeration with respect to propellant C.

Table 6 Summary of experimental and model results for all investigated propellants. Tests are performed between 5 and 25 bar pressure. Pressure is expressed in bar.

	Pocket			Burning rate, mm/s		Radius of collection, μm	
Id	$\overline{R}$, μm	N_p	D_p, μm	Vieille's law	R^2	$R1$ power fitting	R^2
A	162	157	169	$r_b = 1.36\,p^{0.43}$	0.999	$R1 = 655\,p^{-0.42}$	0.832
B	165	180	177	$r_b = 1.29\,p^{0.49}$	0.999	$R1 = 573\,p^{-0.42}$	0.961
C	115	45	110	$r_b = 1.65\,p^{0.40}$	0.952	$R1 = 249\,p^{-0.37}$	1.000
D	347	1263	338	$r_b = 1.43\,p^{0.43}$	0.995	$R1 = 710\,p^{-0.40}$	0.985

The trend is in agreement with the size of the pocket structure.

The power correlation between the radius of collection $R1$ and the pressure (Table 6) features negative exponent, spanning from 0.37 to 0.42. Agglomerate size decreases once the pressure is incremented. The similarity between the modulus of these exponents and the ballistic coefficient n is not supported by any speculation, as of now. If all pressure exponents q are averaged, one obtains $\bar{q} = 0.403 \pm 0.032$ (t-student for 95% probability). All values fall in the confidence interval, suggesting that the dependence of $R1$ from the pressure is approximately uniform, within the monitored conditions and for tested materials. The variation of agglomeration behavior among propellants is recorded by the pre-exponential coefficient z. From a mathematical point of view, z represents the mean CCP size at 1 bar. Specific experimental data are currently not available.

C. Prediction of agglomerate size distributions

The model presented in the previous section can be used to predict the size distribution of a propellant combustion, once the collection radius $R1$ is selected. This information can be obtained by the power fitting after a proper experimental calibration. As a matter of example, the model is applied to propellant A, burning at 20 bar. The relevant power fitting for the radius of collection is available from Table 6 ($R1 = 186\,\mu m$ for the mentioned condition). The code is run on a heterogeneous model of propellant A, generating a list of agglomerates. The comparison of model data and experimental probability density function (PDF) is reported in Figure 13. A cutoff of

75 μm is applied for consistency with the experimental set of data. The matching of the model is satisfactory, considering that only one parameter is used. Good agreement is obtained mainly in the central part of the distribution. The location of the peaks are about 20 μm far from each other. The steep decrement of the PDF, recorded at 175 μm by experiments, is correctly reproduced. Curve comparison highlights some mismatches which can attributed to model simplicity. Larger agglomerates of about 200 μm are not obtained. These particles derive from interpocket agglomeration and their size may depend on the movement capability of the agglomerate on the burning surface. In this perspective, local effects, viscosity of the superficial layer, or position of the agglomerate with respect to the interpocket bridges become important but are not considered in this model. On the left leg of the distribution, a general overestimation is visible, caused by the sensitivity of the experimental methodology and by data cutoff.

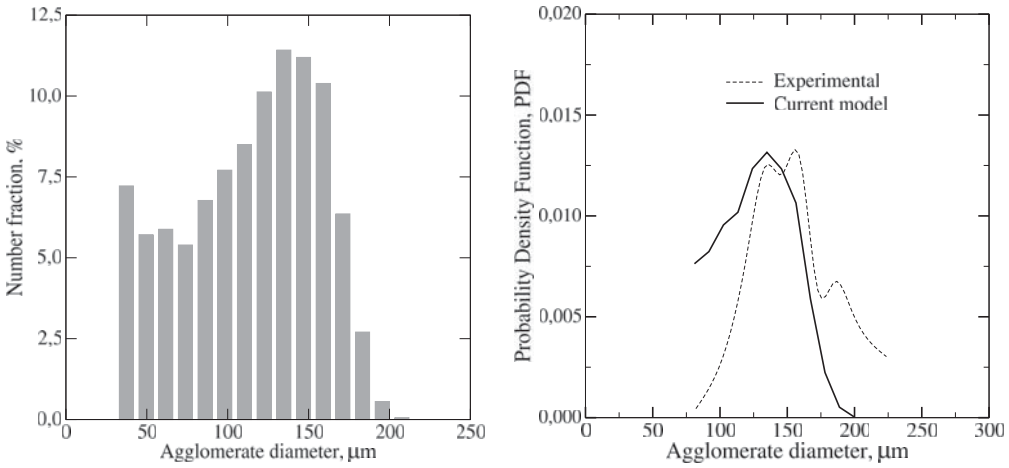

(a) Histograms of model prediction (b) Experimental and numerical PDFs

Fig. 13 Comparison between predicted and experimental agglomerate size distributions for combustion of propellant A at 20 bar.

V. Conclusion

This paper has presented a methodology to analyze solid rocket propellant heterogeneity and, on this basis, to investigate incipient metal fuel agglomeration. The technique grounds on the definition of some geometric properties by using spatial statistical descriptors (e.g. pair correlation function). The analysis is performed on a heterogeneous propellant model, built by a packing code

The initial discussion has addressed representativity of macroscopic properties. The use of a finite number of particles to model propellant heterogeneity introduces variability of the microstructure which reflects on average statistical features. A sensitivity analysis was presented, showing the dependence of mean data scattering from the size of the model propellant.

An algorithm to extract the geometric properties of the average pocket structure was presented. Pocket size and its metal content were derived from the application of two-point spatial statistic functions. The results were compared to experimental distributions of condensed combustion products, after the release from the combustion surface (incipient agglomeration). From the comparison between microstructural geometric properties and experimental data, it was verified that the agglomeration process operated according to interpocket or subpocket regimes, recalling the theoretical interpretations described by Babuk in the open literature. Burning rate and combustion pressure were the drivers.

An agglomeration model that included both geometric pocket features and combustion dependence was presented. The model randomly samples a heterogeneous propellant model and defines the size of the agglomerates by probing the distance of neighboring aluminum particles. The algorithm uses one free parameter, called radius of collection $R1$, to introduce pressure and combustion dependence. Tests on model sensitivity and fitting with four sets of experimental data were proposed. Finally, the detailed results of the agglomeration model were compared to experimental data. Good replication of agglomerate size distribution was observed. Model simplicity caused also some mismatches for the largest agglomerates.

The novelty of this agglomeration model consists in the coupled interaction of microstructure and combustion, introduced by one sole free parameter. The current model shows promising results for aluminum agglomeration, supported by comparison with experimental data and fittings for AP-HTPB-Al propellants. The applicability of the model can be extended to other classes of energetic materials where the three-dimensional microstructure dominates over the combustion process and agglomeration occurs at the burning surface, after accumulation of close particles. Proper experimental tuning of $R1$ dependence is required for different oxidizer and binder. Nonetheless, the simplicity of the model limits the predictive capability to mere geometric considerations. In the

current version, the metal is assumed to be chemically inert during incipient agglomeration. Rather, chemical and physical nature of fuel powders influence the generation of aggregates and may prevent their conversion into agglomerates (e.g. nanometric aluminum or boron-based fine powders). The extension of these kinds of modeling approaches to new metal fuels must include the combustion peculiarities of ingredients. In this respect, high-speed and high-resolution visualizations represent a valuable support to the implementation of new phenomenological models.

Acknowledgments

Computational resources were granted by CINECA consortium. The packing code used in this work is a property of CSAR, University of Illinois at Urbana Champaign. The authors wish to acknowledge Dr. Stefano Dossi from SPLab-POLIMI for his support with thermochemical data.

References

[1] Price, E.W., "Combustion of metallized propellants", *Fundamental of Solid Propellant Combustion*, edited by K.K. Kuo and M. Summerfield, Progress in Astronautics and Aeronautics Series, Vol. 90, AIAA, New York, NY, USA, pp. 479–513, 1984.

[2] DeLuca, L., Galfetti, L., Colombo, G., Maggi, F., Bandera, A., Babuk, V.A., and Sinditskii, V.P., "Microstructure effects in aluminized solid rocket propellants", *Journal of Propulsion and Power*, Vol. 26, No. 4, 2010, pp. 724–733, doi:10.2514/1.45262.

[3] DeLuca, L.T., Galfetti, L., Maggi, F., Colombo, G., Reina, A., Dossi, S., Consonni, D., and M., B., "Innovative Metallized Formulations for Solid Rocket Propulsion", *Chinese Journal of Energetic Materials*, Vol. 20, No. 4, 2012, pp. 465–474, doi:10.3969/j.issn.1006-9941.2012.04.018.

[4] DeLuca, L.T., Marchesi, E., Spreafico, M., Reina, A., Maggi, F., Rossettini, L., Bandera, A., Colombo, G., and Kosowski, B., "Aggregation Versus Agglomeration in Metallized Solid Rocket Propellants", *International Journal of Energetic Materials and Chemical Propulsion*, Vol. 9, No. 1, 2010, doi:10.1615/IntJEnergeticMaterialsChemProp.v9.i1.60.

[5] Maggi, F., Dossi, S., and DeLuca, L. T., "Combustion of metal agglomerates in a solid rocket core flow", *Acta Astronautica*, Vol. 92, 2012, pp. 163–171, doi:10.1016/j.actaastro.2012.04.036.

[6] Reydellet, D., "Performance of rocket motors with metallized propellants", AGARD, Advisory Report AR-230, 1986.

[7] Meyer, R.X., "In-flight formation of slag in spinning solid propellant rocket motors", *Journal of Propulsion and Power*, Vol. 8, No. 1, 1992, pp. 45–50, doi:10.2514/3.23440.

[8] Babuk, V.A., Vasilyev, V.A., and Malakhov, M.S., "Condensed Combustion Products at the Burning Surface of Aluminized Solid Propellant", *Journal of Propulsion and Power*, Vol. 15, No. 6, 1999, pp. 783–793, doi:10.2514/2.5497.

[9] Povinelli, L.A. and Rosenstein, A., "Alumina Size Distributions for High-Pressure Composite Solid-PropellantCombustion", *AIAA Journal*, Vol. 2, No. 10, 1964, pp. 1754–1760, doi:10.2514/3.2660.

[10] Povinelli, L. A., "Effect of oxidizer particle size on additive agglomeration", NASA Technical Note D-1438, 1962.

[11] Maggi, F., Bandera, A., De Luca, L.T., Thoorens, V., Trubert, J.F., and Jackson, T.L., "Agglomeration in Solid Rocket Propellants: Novel Experimental and Modeling Methods", *Progress in Propulsion Physics*, Vol.2, edited by L.T. DeLuca, C. Bonnal, O. Haidn, and S. Frolov, EDP Sciences, pp. 81–98, 2011. doi:10.1051/eucass/201102081

[12] Cohen, N.S., "A Pocket Model for Aluminum Agglomeration in Composite Propellants", *AIAA Journal*, Vol. 21, No. 5, 1983, pp. 720–725, doi:10.2514/3.8139.

[13] Yavor, Y., Gany, A.,and M. W. Beckstead, "Modeling of the agglomeration phenomena in combustion of aluminized composite solid propellant", *Propellant, Explosives, Pyrotechnics*, Vol. 39, No. 2, 2014, pp. 108–116, doi:10.1002/prep.201300073.

[14] Gallier, S., "Microstructure of Composite Propellants Using Simulated Packings and X-Ray Tomography", *Journal of Propulsion and Power*, Vol. 24, No. 1, 2008, pp. 154–157, doi:10.2514/1.30454.

[15] Collins, B., Maggi, F., Matous, K., Jackson, T.L., and Buckmaster, J., "Using Tomography to Characterize Heterogeneous Propellants", *AIAA Paper*, 2008-0941, ,2008.

[16] Rashkovskii, S. A., "Metal Agglomeration in Solid Propellants Combustion - Part 2: NumericalExperiments", *Combustion Science and Technology*, Vol. 136, 1998, pp. 149–169, doi:10.1080/00102209808924169.

[17] Maggi, F., Stafford, S., and Jackson, T.L., "Nature of packs used in propellant modeling", *Physical Review E*, Vol. 77, No. 046107, 2008, pp. 1–17, doi:10.1103/PhysRevE.77.046107.

[18] Maggi, F., Bandera, A., Galfetti, L., DeLuca, L.T., and Jackson, T.L., "Efficient Solid Rocket Propulsion for Access to Space", *Acta Astronautica*, Vol. 66, No. 11-12, 2010, pp. 1563–1573, doi:10.1016/j.actaastro.2009.10.012.

[19] Gallier, S., "A stochastic pocket model for aluminum agglomeration in solid propellants", *Propellant, Explosives, Pyrotechnics*, Vol. 34, No. 2, 2009, pp. 97–105, doi:10.1002/prep.200700260.

[20] Knott, G.M., Jackson, T.L., and Buckmaster, J., "Random Packing of Heterogeneous Propellants", *AIAA Journal*, Vol. 39, No. 4, 2001, pp. 678–686, doi:10.2514/2.1361.

[21] Gordon, S. and McBride, B.S., "Computer Program for Calculation of Complex Chemical Equilibrium Compositions and Applications", NASA RP-1311, 1994.

[22] Beckstead, M.W., Derr, R.L., and Price, C.F., "A Model of Composite Solid-Propellant Combustion Based on Multiple Flames", *AIAA Journal*, Vol. 8, No. 12, 1970, pp. 2200–2207, doi:10.2514/3.6087.

[23] Trunov, M.A., Schoenitz, M., and Dreizin, E.L., "Ignition of Aluminum Powders Under Different Experimental Conditions", *Propellants, Explosives, Pyrotechnics*, Vol. 30, No. 1, 2005, pp. 36–43. doi:10.1002/prep.200400083

[24] Pokhil, P.F., Belyaev, A.F., Frolov, Y.V., Logachev, V., and Korotkov, A., "Combustion of Metal Powders in Active Media", Defense Technical Information Center, Technical Report AD0769576, 1972.

[25] Mullen, J.C. and Brewster, M.Q., "Characterization of aluminum at the surface of fine AP-HTPB composite propellants", *AIAA Paper*, No. 2008-5259, 2008.

[26] Dossi, S., Reina, A., Maggi, F., and De Luca, L., "Innovative Metal Fuels for Solid Rocket Propulsion", *International Journal of Energetic Materials and Chemical Propulsion*, Vol. 11, No. 4, 2012, pp. 299–322. doi:10.1615/IntJEnergeticMaterialsChemProp.2013005748

[27] Steinz, J. A., Stang, P. L., and Summerfield, M., "The Burning Mechanism of Ammonium Perchlorate-Based Composite Solid Propellants", Department of Aerospace and Mechanical Sciences, Technical Report 830, Princeton University, Princeton, USA, 1969.

[28] Miller, R. R., "Effects of particle size on reduced smoke propellant ballistics", *AIAA Paper*, No. 82-1096, 1982.

[29] Stoyan, D. and Stoyan, H., *Fractals, random shapes and point fields*, Wiley series in probability and mathematical statistics, Wiley, Chirchester, England, 1994.

[30] Kumar, N.C., Matous, K., and Geubelle, P.H., "Reconstruction of Periodic Unit Cells of Multimodal Random Particulate Composites Using Genetic Algorithms", *Computational Materials Science*, Vol. 42, 2008, pp. 352–367, doi:10.1016/j.commatsci.2007.07.043.

[31] Bandera, A., Maggi, F., and DeLuca, L. T., "Agglomeration of Aluminized Solid Rocket Propellants", *AIAA Paper* No. 2009-5439, 2009.

[32] Bandera, A., "Combustion of Metallized Solid Rocket Propellants and Motor Performance", Ph.D. Dissertation, Aerospace Engineering Dept., Politecnico di Milano, Milan, Italy, 2009.

[33] *OpenMP Application Program Interface*, Ver. 2.5, 2005.

[34] *MPI: A message passing interface standard*, Ver. 1.1, 2003.

[35] Kochevets, S., Buckmaster, J., Jackson, T. L., and Hegab, A., "Random Packs and Their Use in Modeling Heterogeneous Solid Propellant Combustion", *Journal of Propulsion and Power*, Vol. 17, No. 4, 2001, pp. 883–891, doi:10.2514/2.5820.

[36] Maggi, F., Jackson, T. L., and Buckmaster, J., "Aluminum agglomeration modeling using a packing code", *AIAA Paper* No. 2008-0940, 2008.

[37] Galassi, M., Davies, J., Theiler, J., Gough, B., andM. Booth, G. J., and Rossi, F., "GNU Scientific Library Reference Manual", Technical Report 1.6, GNU, 2004.